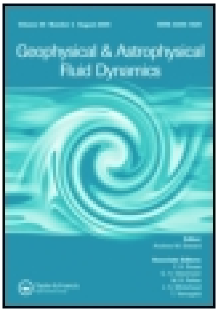

Geophysical & Astrophysical Fluid Dynamics
Publication details, including instructions for authors and subscription information:
http://www.tandfonline.com/loi/ggaf20

Small-scale hydromagnetic flow in the Earth's core: Rise of a vertical buoyant plume

David E. Loper [a] & H. Keith Moffatt [b]
[a] Geophysical Fluid Dynamics Institute, Florida State University, Tallahassee, Florida, USA
[b] Department of Applied Mathematics and Theoretical Physics, University of Cambridge, Cambridge, UK
Published online: 19 Aug 2006.

To cite this article: David E. Loper & H. Keith Moffatt (1993) Small-scale hydromagnetic flow in the Earth's core: Rise of a vertical buoyant plume, Geophysical & Astrophysical Fluid Dynamics, 68:1-4, 177-202, DOI: 10.1080/03091929308203567

To link to this article: http://dx.doi.org/10.1080/03091929308203567

Geophys. Astrophys. Fluid Dynamics, Vol. 68, pp. 177–202
Reprints available directly from the publisher
Photocopying permitted by license only

SMALL-SCALE HYDROMAGNETIC FLOW IN THE EARTH'S CORE: RISE OF A VERTICAL BUOYANT PLUME

DAVID E. LOPER

Geophysical Fluid Dynamics Institute, Florida State University, Tallahassee, Florida, USA

H. KEITH MOFFATT

Department of Applied Mathematics and Theoretical Physics, University of Cambridge, Cambridge, UK

(Received 22 October 1991; in final form 28 April 1992)

The steady and transient flow induced by a vertical cylinder of buoyant electrically conducting fluid immersed in an infinite extent of slightly denser fluid in the presence of a horizontal magnetic field is investigated, with the aim of elucidating the small-scale flow within the Earth's core. The evolution from a state of rest may be divided into three regimes. For short times [$t < O(L^2\mu\sigma)$ where L is the horizontal scale of the plume] Alfvén waves propagate a distance $V_A t$ along the magnetic field lines, accelerating the fluid to a speed of order $(\Delta\rho)gL/\rho V_A$ where $V_A = B/(\rho\mu)^{1/2}$ is the Alfvén speed and $\Delta\rho$ is the density deficit of the buoyant plume. For intermediate times [$O(L^2\mu\sigma) < t < O(L^2/\nu)$] lateral ohmic diffusion becomes important and the rise speed and lateral extent grow as the square-root of time: $O[(\Delta\rho g/B)(t/\rho\sigma)^{1/2}]$ and $O[LB(\sigma t/\rho)^{1/2}]$, respectively. For large times [$t > O(L^2/\nu)$] lateral viscous diffusion also becomes important and a quasi-steady state is reached having rise speed of order $(\Delta\rho)gL/B(\rho\sigma\nu)^{1/2}$ and lateral extent of order $L^2B(\sigma/\rho\nu)^{1/2}$. For values of parameters thought to be relevant to the core, the short-time solution lasts roughly an hour and the intermediate-time solution lasts several decades. The long-time solution may not be relevant to the core as the fluid can rise to the top during the intermediate-time regime. The rise speeds associated with this plume flow may exceed those estimated from secular variation, but this result is sensitive to the size of the density deficit, which is poorly known, and to the particular orientation of the plume that has been chosen.

KEY WORDS: Earth's core, buoyant plume, hydromagnetic flow.

1. INTRODUCTION

It is now widely accepted that the Earth's magnetic field is powered by self-exciting dynamo action associated with fluid motion in the liquid outer core. The most plausible drive for this motion is compositional convection associated with the cooling of the Earth and the slow solidification of the inner core (Braginsky, 1963; Lowes, 1984). As the liquid iron alloy, of which the outer core is composed, freezes onto the inner core, an excess of the lighter elements remains in the surrounding liquid, driving the convective motions.

The compositionally buoyant fluid which drives the convective flow may be generated within a 'mushy zone' at the top of the inner core (Loper and Roberts, 1981; Loper, 1983). This zone is a layer of dendritic metallic crystals which serves to circumvent the rate-limiting process of compositional diffusion and allows solidification to proceed more rapidly than at a non-convoluted interface. This layer, which has an effective thickness of about 1 km, behaves as a porous medium, within which buoyant fluid, having a density deficit relative to the overlying fluid, is continuously generated. Model experiments involving freezing of an aqueous solution of ammonium chloride (Copley, *et al.*, 1970; Roberts and Loper, 1983) indicate that the fully developed convective flow can take the form of plumes of buoyant fluid emanating from the mushy zone via vertical 'chimneys' that form spontaneously within it. Alternatively the flow may take the form of rising individual parcels of buoyant material, possibly entraining ambient liquid in the process (Moffatt, 1989). Moreover, it must be admitted that conditions in the high-pressure liquid-metal environment near the inner core boundary (ICB) are so utterly different from those of the model experiments that the preferred pattern of convection may be quite different from that just described. Nevertheless, it is very likely that the buoyant fluid generated near the ICB will rise through the overlying liquid outer core.

Very little is known about the dynamics of small-scale buoyant plumes and parcels in a rotating hydromagnetic environment. Even such fundamental properties as the direction and rate of rise are unknown. In the complex interplay of Coriolis, Lorentz and buoyancy forces, it is not possible to estimate with confidence the rate of rise of the buoyant fluid by means of a crude force balance. The goal of this, and subsequent, papers is to quantify the direction and rate of rise of buoyant parcels and plumes within the outer core of the Earth, and to identify the spatial scales of the flow structures associated with them. The ultimate goal is a better understanding of the flow structures associated with the dynamo process and of the dynamical structure of the outer core.

In the present paper we will concentrate on the relatively simple problem of the flow of a cylindrical plume of buoyant fluid emanating from a chimney in the polar region of the inner core and rising parallel to the axis of rotation (see Figure 1). We shall assume that rotation and gravity vectors are uniform, constant and anti-parallel

$$\boldsymbol{\Omega}=\Omega\hat{\mathbf{z}}\,, \qquad \mathbf{g}=-g\hat{\mathbf{z}}\,,$$

and that the magnetic field vector, sustained by large-scale dynamo action, is nearly uniform on the small scale of the plume:

$$\mathbf{B}=B\hat{\mathbf{x}}+C\hat{\mathbf{z}}+\text{a perturbation}\,.$$

With the chosen geometry the flow is entirely in the vertical direction. Consequently the vertical component of the magnetic field has no dynamical effect. For simplicity in what follows we shall therefore set $C=0$. The imposed field is then

$$\mathbf{B}_0=B\hat{\mathbf{x}}\,.$$

The buoyancy is assumed to be compositional in origin; we will neglect thermal effects. Furthermore, compressibility will be ignored, so that the density of the fluid depends only on its composition. We shall assume that this flow is the smallest scale of motion, so that there is no turbulent motion on a smaller scale which produces eddy diffusivities; diffusion is governed by the molecular diffusivities. Also, molecular material diffusivity is assumed to be negligibly small, so that the composition and density of a fluid parcel remains constant. That is,

$$\rho = \rho_0 - \Delta\rho ,$$

where $\Delta\rho$ is prescribed for each parcel. Note that $\Delta\rho > 0$ for buoyant material.

The chosen configuration is mathematically both simple and singular in three respects. First, since the flow is assumed to be one dimensional and parallel to the axis of rotation, the inertial and Coriolis forces are identically zero. Second, since the flow is assumed to be parallel to the surface of the buoyant material, that surface is not deformed by the flow. Third, as we shall see in the subsequent analysis, the rise speed in this configuration can be anomalously large.

The difficulty of quantifying the rate of rise may be appreciated by considering the relatively simple problem of the (nonrotating) flow of an electrically conducting fluid in a pipe in the presence of a strong transverse magnetic field driven by a prescribed pressure gradient. In the notation of this paper, equation (17) of Shercliff (1956) quantifies the flow up a circular pipe as

$$w = \frac{Mk}{1+\gamma Mk} ,$$

where w is the dimensionless flow speed, M is the Hartmann number based on the lateral size of the pipe [defined by (2.5)], k is the dimensionless local half-width of the pipe (in the direction of the applied field) and γM is the ratio of the conductance of the pipe wall to that of the adjacent Hartmann layer. Note that k is a function of the coordinate normal to the plane of the flow and field. Typically $M \gg 1$ and $k = O(1)$. For an insulating wall, $\gamma = 0$ and $w = Mk$; the flow speed is large and varies as k. If $\gamma = O(1)$, then $\gamma M \gg 1$ and $w = 1/\gamma$; the flow speed (outside the Hartmann layers) is of unit order and uniform. Note that a relatively small amount of wall conductance strongly affects the magnitude and structure of the flow.

The disparity of flow speed in Shercliff's problem can be traced to the return pathways available for the electric current, driven by crossing the axial flow in the pipe (forced by the pressure gradient) with the transverse magnetic field. This current serves to transfer the force of the pressure gradient to the pipe wall. If a return path is available for the current through the conducting pipe wall, the transfer of force is efficient and the flow speed is 'normal', but if the return path is entirely through the narrow Hartmann layer, the transfer is inefficient and the flow speed becomes large. This coupling problem has some similarity to that between the core and mantle, with the spin-up time being affected by a relatively small amount of mantle conductivity (see Loper, 1971). Note that the flow speed is uniform if the fluid and pipe are electromagnetically coupled, but is variable for the weaker viscous coupling.

The problem considered below has some similarity with the pipe-flow problem, even though it is an unbounded free-convection flow, rather than a confined pressure-driven flow. As in the pipe-flow problem, the vertical flow (now forced by buoyancy) crossed with the transverse magnetic field drives a flow of current in the third direction, but now there is no fixed rigid conducting boundary through which the return current can flow. Consequently the buoyancy force is not efficiently balanced and the rate of flow can become large. We wish to quantify this flow rate, and the associated spatial structures, in both steady and time-developing flows.

2. DEVELOPMENT OF GOVERNING EQUATIONS

We consider a viscous, incompressible, electrically conducting fluid of variable non-diffusing density, governed by the following equations:

$$\begin{gathered} \rho D\mathbf{u}/Dt + 2\rho\boldsymbol{\Omega}\times\mathbf{u} = -\nabla p + \mu^{-1}(\nabla\times\mathbf{B})\times\mathbf{B} + \rho\mathbf{g} + \rho\nu\nabla^2\mathbf{u}\,, \\ \partial\mathbf{B}/\partial t = \nabla\times(\mathbf{u}\times\mathbf{B}) + (\sigma\mu)^{-1}\nabla^2\mathbf{B}\,, \\ D\rho/Dt = 0\,, \qquad \nabla\cdot\mathbf{B} = 0\,, \qquad \nabla\cdot\mathbf{u} = 0\,. \end{gathered} \tag{2.1}$$

The notation is standard; see Roberts (1967).

The first task is to nondimensionalize the equations. This is not a trivial exercise for, as we noted previously and shall see below, the order of magnitude of the velocity varies strongly with time. Let us assume a dominant balance between buoyancy and Lorentz force (in the case that the Coriolis force is inactive) and between magnetic induction and diffusion. This leads to a velocity scale of $W_0 = (\Delta\rho)g/\sigma B^2$ and a magnetic-perturbation scale of $BW_0L\sigma\mu$ where L is a measure of the lateral scale of the buoyant plume. The time scale is chosen so that the Alfvén speed is unity: $T_0 = (\mu\rho)^{1/2}L/B$. Altogether

$$\begin{gathered} \mathbf{u} = W_0 w^*\hat{\mathbf{z}}\,, \qquad \mathbf{B} = B\hat{\mathbf{x}} + (BW_0L\sigma\mu)c^*\hat{\mathbf{z}}\,, \\ \nabla = \nabla^*/L\,, \qquad \partial/\partial t = (T_0)^{-1}\partial/\partial t^*\,, \end{gathered} \tag{2.2}$$

and

$$p = p_0 - \rho_0 gz + W_0 L\sigma B^2 p^*\,.$$

z is the upward coordinate, parallel to the plume, x is the horizontal coordinate in the direction of the applied field, and y is the coordinate normal to the plane of the plume and the applied field; see Figure 1. In what follows the spatial scale in the direction of the applied field will be referred to as the length and that normal to the flow and field will be called the width.

With the chosen geometry, we may consistently assume that the density perturbation $\Delta\rho$ depends only on the horizontal coordinates and the dimensionless

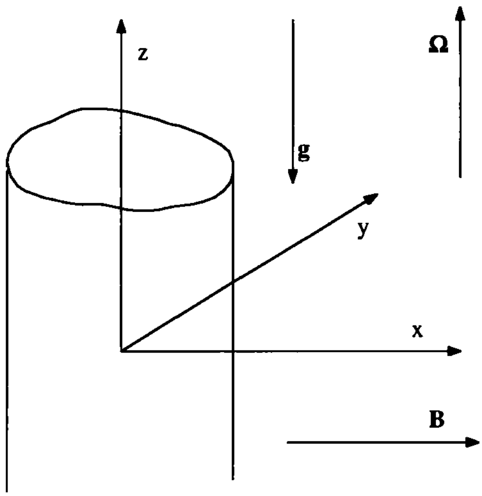

Figure 1 Three-dimensional orientation of the buoyant cylinder of fluid with respect to the applied gravitational (**g**), rotational (**Ω**) and magnetic field (**B**) vectors and with respect to the Cartesian coordinates, x, y, z.

variables w^*, c^* and p^* are functions of the horizontal coordinates and time. The equation governing the transport of density, the continuity equations and the horizontal components of the momentum and magnetic diffusion equations are automatically satisfied [with $p^* = -W_0 L\sigma\mu(c^*)^2/2$]. The remaining equations are, upon dropping the asterisks,

$$M^{-2}\nabla^2 w - (MP)^{-1} w_t + c_x = -f(x, y)\ , \tag{2.3}$$

and

$$\nabla^2 c - (MP)c_t + w_x = 0\ , \tag{2.4}$$

where

$$M = LB(\sigma/\rho_0 \nu)^{1/2}\ , \qquad \text{and} \qquad P^2 = \sigma\mu\nu\ . \tag{2.5}$$

Here M is the Hartmann number, P^2 is the magnetic Prandtl number, $f = (\Delta\rho)/(\Delta\rho)_{\max}$, $\nabla^2 = \partial^2/\partial x^2 + \partial^2/\partial y^2$ and subscripts denote partial differentiation. We shall consider only situations in which $f = 0$ or 1.

We shall assume the following parameter values for the lower portion of the outer core of the Earth: $\rho_0 = 10^4$ kg/m^3, $g = 3$ m/s^2, $\sigma = 3 \times 10^5$ /Ωm, $\mu = 4\pi \times 10^{-7}$ H/m, $B = 2 \times 10^{-2}$ T, $\nu = 10^{-5}$ m^2/s, $\Delta\rho = 10^{-3}$ kg/m^3. The first four of these are reasonably well known while the latter three are quite uncertain. We have assumed a large toroidal magnetic field ($B = 200$G); the value may easily be smaller by a factor of 2 or 4. The value of the viscosity of the core may be larger by one or more orders of magnitude (Gans, 1972). Moffatt (1989) estimated the average value of $\Delta\rho$ in the core to be 3×10^{-5} kg/m^3. We have chosen a value 30 times larger, assuming that only a few percent of the material in the core is buoyant. Nevertheless the relative size of the density perturbation is very small: $\Delta\rho/\rho=10^{-7}$.

With these estimates $P(=2\times10^{-3})$ is much smaller than one and, for any plume larger than 3 mm in horizontal extent, M is larger than one; typically M is very large. Also, note that the Lundquist number MP, measuring the relative sizes of inertial and Lorentz forces, is large for any plume greater than about 14 m in horizontal extent. The velocity scale W_0 is only 2.5×10^{-8} m/s, far smaller than the value of 10^{-4} m/s typically quoted from secular variation. However, we shall see that the actual flow speed attained in the vertical plume easily exceeds the latter speed. The magnetic Reynolds number of the flow,

$$R_m=W_0L\sigma\mu=(\Delta\rho)g\mu L/B^2\ ,$$

is small for any plume having a lateral scale smaller than about 10^5 m.

Note that the magnetic field variable c is in effect a stream function for the electric current which flows in the horizontal plane:

$$\mathbf{j}=BW_0\sigma[c_y\hat{\mathbf{x}}-c_x\hat{\mathbf{y}}]\ . \tag{2.6}$$

Equations (2.3) and (2.4) are equivalent to (8) and (9) of Shercliff (1956), except that the magnitudes of the dependent variables have been chosen differently. As in Shercliff's case, these equations admit Hartmann-layer modes having narrow lateral scale of order $1/M$. However, they admit a second mode which is missing in the pipe-flow problem because of the confined geometry, but which plays an important role in the following analysis. To see how this mode arises, consider the single scalar operator formed by combining the steady homogeneous versions of (2.3) and (2.4):

$$\left(\frac{\nabla^4}{M^2}-\frac{\partial^2}{\partial x^2}\right)(c,w)=0\ .$$

The familiar Hartmann mode has both ∇ and $\partial/\partial x=O(M)$. The new mode has $\partial/\partial y=O(1)$ and $\partial/\partial x=O(1/M)$, making it elongated in the direction of the applied magnetic field. This mode is analogous to the Taylor-column mode in rotating fluids (Moore and Saffman, 1969). In the limit $M\to\infty$, the equations dictate that $\partial/\partial x=0$, in direct analogy with the Taylor-Proudman theorem. The elongation serves to weaken the Lorentz force to a magnitude equal to the viscous force.

This mode was apparently first identified independently by Braginsky (1960) and Hasimoto (1960); we shall refer to it as the Braginsky-Hasimoto mode, or the BH mode, for short. [The equations governing this mode were earlier presented by Lehnert (1952), Shercliff (1953) and Chester (1957) but only in situations which did not reveal this mode.] Letting $x=M\xi$, the equations governing the BH mode are

$$w_{yy}+Mc_\xi=0\ ,\qquad\text{and}\qquad Mc_{yy}+w_\xi=0\ . \tag{2.7}$$

From these it follows that w is larger than c by a factor of M, suggesting that the upward speed in the BH mode is very large. We shall see that this is indeed the case.

The Hartmann-layer modes typically exist adjacent to rigid boundaries to satisfy continuity of velocity and stress. In the absence of rigid boundaries, as is the case here, any instantaneous variation of velocity on a narrow scale excites Alfvén waves which transport the variation along the magnetic field lines, leaving a smoothly varying velocity. Consequently, we anticipate the absence of Hartmann-layer modes in the solution to the present problem. However, the BH mode is present and important, as it carries the return electric current discussed in the introduction.

3. STEADY RISE

The buoyancy of the plume is an applied force which must be transmitted via hydromagnetic interaction or viscosity to a fixed boundary if a precisely steady solution is to exist. Alternatively, the flow may evolve with time. However, in analogy with the rise of a buoyant body in creeping flow, a steady solution can be found for which the momentum of the flow field is infinite. Any time-dependent flow may be expected to evolve toward this solution as time increases. It is in this spirit that we seek a steady solution to the present problem. It is noteworthy that the presence of the magnetic field makes our cylindrical problem well-posed; in its absence, there is no solution (Lamb, 1932, art. 341).

Let us consider a 'top-hat' density distribution for the cylindrical plume; let f be unity for $r<R$ and zero for $r>R$, where $R(\theta)$ is continuous and positive in $-\pi<\theta<\pi$. Here r and θ are standard cylindrical (polar) coordinates; see Figure 2. Further

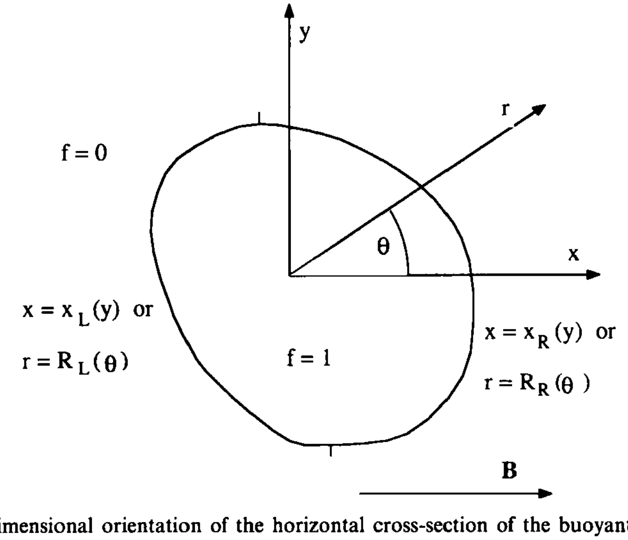

Figure 2 Two-dimensional orientation of the horizontal cross-section of the buoyant cylinder of fluid with respect to the Cartesian coordinates x, y and the polar coordinates r, θ. The buoyant fluid, having $f=1$, is confined within the interior region $r<R(\theta)$, while the non-buoyant exterior [lying in $R(\theta)<r$] is characterized by $f=0$. The right-hand portion of the boundary between interior and exterior is denoted by $x_R(y)$ or $R_R(\theta)$; the left hand portion is denoted by $x_L(y)$ or $R_L(\theta)$.

assume that $R=O(1)$, $M\gg 1$ and $(dR/d\theta)\tan\theta+R=0$ only for two isolated values of θ. The last of these assumptions implies that the lines of the imposed magnetic field cut the boundary of the plume at most twice and that they are parallel to the boundary only at two isolated points, characterized by the maximum and minimum values of y. This assumption, made for mathematical and conceptual simplicity, could be relaxed.

The steady governing equations are

$$M^{-2}\nabla^2 w+c_x=u[r-R(\theta)]-1, \tag{3.1}$$

$$\nabla^2 c+w_x=0\ , \tag{3.2}$$

where u is the heaviside step function $[u(\zeta)=0$ if $\zeta<0$ and $=1$ if $0<\zeta]$. The boundary conditions are:

$$\text{at}\qquad r=R(\theta),\qquad c,\ w,\ c_n \text{ and } w_n \text{ are continuous} \tag{3.3}$$

where n is the normal coordinate in the direction of $\hat{\mathbf{r}}-R_\theta\hat{\boldsymbol{\theta}}$, and

$$\text{as}\qquad r\to\infty,\qquad c,\ w\to 0\ . \tag{3.4}$$

A difficulty in solving the steady problem is to determine the magnitude of the flow. In the interior region ($r<R$, denoted by superscript I) where $f=1$ the governing equations simplify at leading order in powers of M^{-1} to

$$c^I{}_x=-1\ ,\qquad \nabla^2 c^I+w^I{}_x=0\ . \tag{3.5}$$

The first of these determines that $c^I=O(1)$, but the second leaves the magnitude of w^I undetermined. The equations (2.7) governing the BH mode indicate that $w=O(Mc)$, and the boundary conditions require continuity of the variables. (Recall that the Hartmann modes are absent.) Consequently we anticipate that $w=O(M)$ in the interior region. Now the dominant-order solution to (3.5) may be expressed as

$$c^I=-x+h(y)\ ,\qquad \text{and}\qquad w^I=Mk(y)\ , \tag{3.6}$$

where h and k are unit-order functions to be determined. [The particular solution of the second of (3.5) is of smaller order.]

The exterior solution (for $R<r$, denoted by superscript E) consists of the BH mode. The variables in this mode may be rescaled as

$$w^E(x,y)=M\bar{w}(\xi,y)\qquad \text{and}\qquad c^E(x,y)=\bar{c}(\xi,y) \tag{3.7}$$

where $\xi=x/M$. To dominant order in M the exterior equations are

$$\bar{w}_{yy}+\bar{c}_\xi=0\ ,\qquad \bar{c}_{yy}+\bar{w}_\xi=0\ . \tag{3.8}$$

With this scaling, the "inner region" containing the plume collapses to $\xi=0$. For $0<\xi$ decaying modes are characterized by $\bar{w}+\bar{c}=0$ and governed by

$$\bar{w}_{yy}=\bar{w}_{\xi}\ , \tag{3.9}$$

while for $\xi<0$, $\bar{w}-\bar{c}=0$ and

$$\bar{w}_{yy}=-\bar{w}_{\xi}\ . \tag{3.10}$$

These equations are identical to Oseen's equation for slow viscous flow [e.g., see Eq. (20), p. 611 of Lamb, 1932]. However, Oseen's equation applies to transverse motion of a cylinder, not the parallel motion considered here.

Continuity of velocity at the plume boundary requires that $\bar{w}(0,y)=k(y)$. The solution satisfying this condition is:

$$\bar{w}(\xi,y)=-\operatorname{sgn}(\xi)\bar{c}(\xi,y)=\frac{1}{2\sqrt{\pi|\xi|}}\int_{-\infty}^{\infty}k(\eta)\exp\left[-\frac{(y-\eta)^2}{4|\xi|}\right]d\eta\ . \tag{3.11}$$

Continuity of $\bar{c}$ at $r=R$ requires that $\bar{c}^I\pm\bar{w}^I=0$ at $x=x_L$ and x_R, respectively, i.e.,

$$0=x_L-h+k\ , \qquad 0=x_R-h-k\ , \tag{3.12}$$

where

$$x_r=(R_R{}^2-y^2)^{1/2} \qquad \text{and} \qquad x_L=-(R_L{}^2-y^2)^{1/2}\ , \tag{3.13}$$

R_R and R_L being the right-hand and left-hand values of R at a specified value of y (Figure 2). To dominant order in M, continuity of ∇w and ∇c are automatically satisfied by the lack of Hartmann layers. The solution of (3.12) is

$$h=[x_R+x_L]/2=[(R_R{}^2-y^2)^{1/2}-(R_L{}^2-y^2)^{1/2}]/2\ , \tag{3.14}$$

$$k=[x_R-x_L]/2=[(R_R{}^2-y^2)^{1/2}+(R_L{}^2-y^2)^{1/2}]/2\ . \tag{3.15}$$

Note that h is the local center of the plume and k is the local half-width. When necessary k will be assumed to be zero at values of y for which x_R and x_L are undefined (i.e., outside the plume).

It is instructive to verify that the flux of electric current is continuous across the boundary of the buoyant plume, and thus provide a validation of the solutions (3.6) and (3.11). We will consider only the right-hand portion of the boundary, denoted by

$$x-x_R(y)=\text{constant};$$

the analysis of the left-hand portion is identical. The local normal vector is

$$\mathbf{n}=\hat{\mathbf{x}}-(dx_R/dy)\hat{\mathbf{y}}\ . \tag{3.16}$$

Using (2.6) and (3.16) we may write

$$\mathbf{j}\cdot\mathbf{n}=BW_0\sigma j_n \tag{3.17}$$

where

$$j_n=\frac{\partial c}{\partial y}+\frac{dx_R}{dy}\frac{\partial c}{\partial x}. \tag{3.18}$$

We wish to show that j_n is continuous across the plume boundary.

Using (3.6), (3.14) and (3.15) the flow of current from the interior of the plume may be expressed as

$$j_n^I=-dk/dy. \tag{3.19}$$

To find the flow of current to the exterior of the plume, we must use (3.11) evaluated as $\xi\to 0$. It may be shown that the x derivative of this expression is small, of order $1/M$. Consequently only the y derivative in (3.18) contributes to the current flow exterior to the plume. Now

$$\frac{\partial c^E}{\partial y}(\xi,y)=\frac{-1}{2\sqrt{\pi\xi}}\int_{-\infty}^{\infty}k(\eta)\frac{\partial}{\partial y}\exp\left[-\frac{(y-\eta)^2}{4\xi}\right]d\eta=\frac{1}{2\sqrt{\pi\xi}}\int_{-\infty}^{\infty}k(\eta)\frac{\partial}{\partial\eta}\exp\left[-\frac{(y-\eta)^2}{4\xi}\right]d\eta.$$

or integrating by parts and changing variables,

$$\frac{\partial c^E}{\partial y}(\xi,y)=\frac{-1}{2\sqrt{\pi\xi}}\int_{-\infty}^{\infty}\frac{dk}{d\eta}(\eta)\exp\left[-\frac{(y-\eta)^2}{4\xi}\right]d\eta=\frac{-1}{\sqrt{\pi}}\int_{-\infty}^{\infty}\frac{dk}{dy}(y+2\sqrt{\xi}z)\exp[-z^2]dz.$$

In the limit $\xi\to 0$, the integral is simply evaluated:

$$j_n^E=\lim_{\xi\to 0}\left[\frac{\partial c^E}{\partial y}(\xi,y)\right]=-\frac{dk}{dy}(y). \tag{3.20}$$

Equations (3.19) and (3.20) are identical, ensuring continuity of flow of electric current.

As noted by Braginsky (1960), the solution for $\bar{w}(\xi,y)$ is functionally identical to that for the flow of heat in an infinitely long rod with the ξ direction (i.e., the direction of the magnetic field) being the time-like variable (more precisely $|\xi|$ acts as time) and the velocity distribution prescribed at the plume $[\bar{w}=k(y)]$ playing the role of the initial temperature distribution. It follows from this that the integral

$$\int_{-\infty}^{\infty}\bar{w}(\xi,y)dy=\int_{-\infty}^{\infty}k(y)dy \tag{3.21}$$

is a constant independent of ξ and that the momentum of the flow is infinite. Note that the integral of k in (3.21) is equal to half the cross-sectional area of the plume.

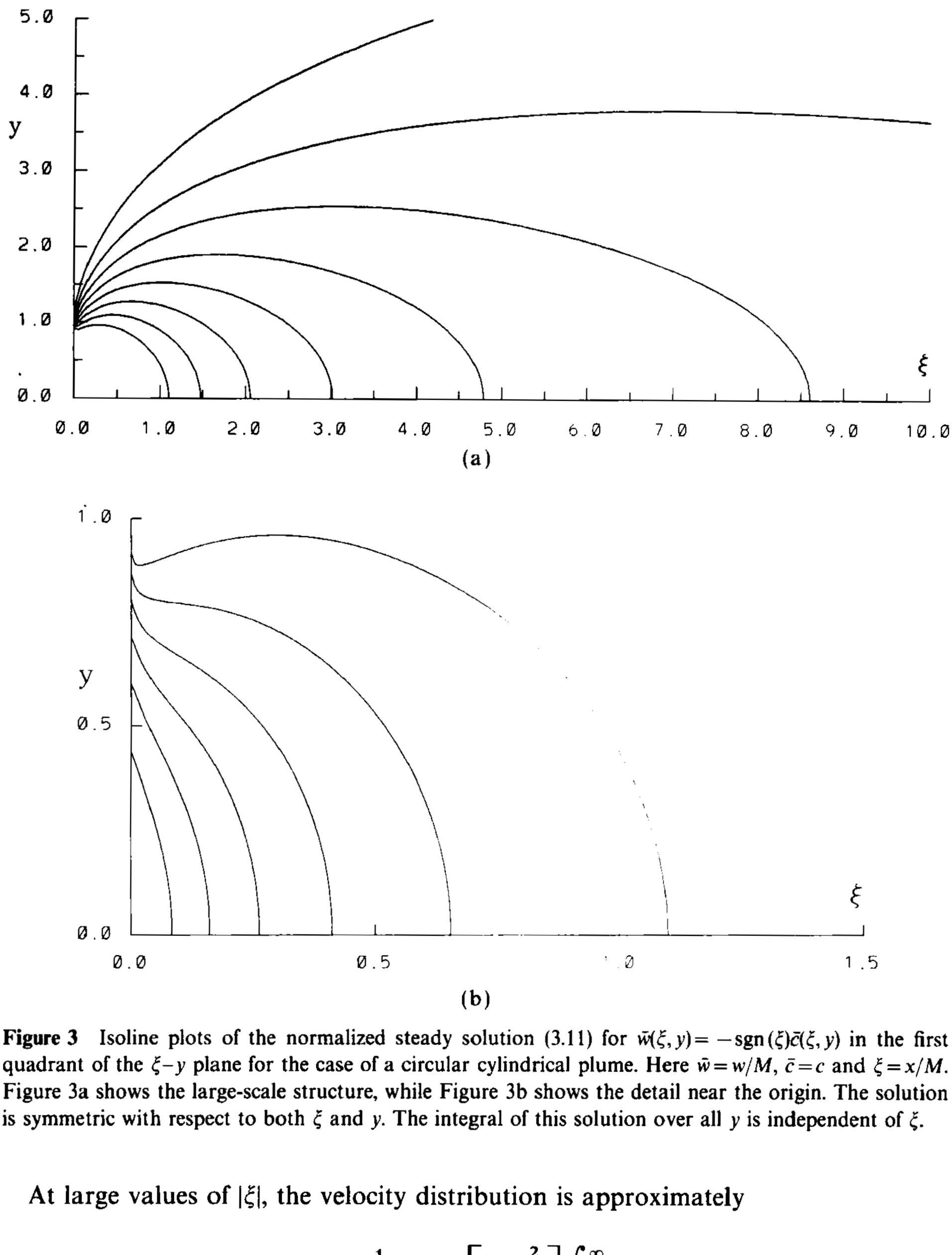

Figure 3 Isoline plots of the normalized steady solution (3.11) for $\bar{w}(\xi, y) = -\operatorname{sgn}(\xi)\bar{c}(\xi, y)$ in the first quadrant of the ξ–y plane for the case of a circular cylindrical plume. Here $\bar{w} = w/M$, $\bar{c} = c$ and $\xi = x/M$. Figure 3a shows the large-scale structure, while Figure 3b shows the detail near the origin. The solution is symmetric with respect to both ξ and y. The integral of this solution over all y is independent of ξ.

At large values of $|\xi|$, the velocity distribution is approximately

$$\bar{w}(\xi, y) \approx \frac{1}{2\sqrt{\pi|\xi|}} \exp\left[-\frac{y^2}{4|\xi|}\right] \int_{-\infty}^{\infty} k(\eta)\, d\eta \,. \tag{3.22}$$

This solution is equivalent to that given in (1.14) of Braginsky (1960) and in (3.7′) of Hasimoto (1960). Note the slow rate of decay of the velocity with distance along the magnetic field (i.e., in the ξ direction) at constant y.

For $|\xi| \ll 1$ (i.e., $|x| \ll M$), (3.11) simplifies to

$$\bar{w}(0, y) = -\operatorname{sgn}(\xi)\bar{c}(0, y) = k(y) . \tag{3.23}$$

Thus the flow induced in the vicinity of a buoyant cylinder of fluid aligned with gravity and rotation consists of planar sheets of uniform upward flow, lying in the plane of the plume and the applied magnetic field. The speed of a specific sheet is directly proportional to the length (in the direction of the applied field) of the buoyant plume which this sheet intersects, and the width of the region of upward flow is identical to that of the buoyant cylinder.

Isolines of upward flow plotted in the $\xi - y$ plane coincide with the streamlines of the electric current, as noted by Hasimoto (1960). These isolines are plotted in Figure 3 for a plume of circular cross-section $[k=(1-y^2)^{1/2}]$. In this case

$$w = M\sqrt{1-y^2} . \tag{3.24}$$

The dimensional rise speed of a vertically oriented buoyant cylinder is, from (3.6), for large M

$$w_d = \frac{(\Delta\rho)gL}{B\sqrt{\rho_0 \nu\sigma}} . \tag{3.25}$$

This speed is larger by a factor M than that anticipated from simple scaling arguments. Note that this rise speed tends to infinity as B tends to zero; the nonmagnetic problem is singular. It is of interest to determine the manner and time scale for establishment of this rapid upward flow.

4. TIME DEVELOPMENT

The equations governing the time development of the flow induced by a cylindrical plume of buoyant fluid having the top-hat buoyancy distribution are (2.3) and (2.4) with $f = 1 - u[r - R(\theta)]$. These are subject to boundary conditions (3.3) and (3.4). We shall assume that the initial state is one of no motion and no electric current:

$$w(x, y, 0) = c(x, y, 0) = 0 . \tag{4.1}$$

Note that the buoyancy force supplies momentum at a rate MP, so that the total momentum of the flow varies as $MPAt$, where

$$A = \int_{-\infty}^{\infty} 2k(y)dy \tag{4.2}$$

is the cross-sectional area of the plume. This momentum is fed to flow structures extending from the plume along the magnetic field in both directions. The momentum for each increases as $MPAt/2$.

For very short times the buoyant fluid within the plume accelerates (relatively) rapidly from rest while the non-buoyant exterior fluid remains at rest: $w^I = MPt$ and $w^E = 0$. The discontinuity in velocity thus induced is propagated along the magnetic field lines as Alfvén waves which travel at unit dimensionless speed. These waves traverse the buoyant region in time of order unity, leaving an upward flow of magnitude MP. Since $P \ll 1$, this flow speed is considerably less than that found in the steady state.

4.1 *Short-time regime: two-dimensional Alfvén mode* ($t \ll MP$)

Once the Alfvén waves traverse the buoyant region, the rapid acceleration ceases and a quasi-steady situation prevails near the plume. Within the plume the buoyancy force is balanced by the Lorentz force, and acceleration there is zero to dominant order. An electric current of density $(\Delta\rho)g/B$ flows laterally (in the $+y$ direction) within the buoyant plume. This electric current, when crossed with the applied magnetic field produces a downward force which exactly counterbalances the buoyancy force. The total electric current flowing in the cross-stream direction (y) has a magnitude $[(\Delta\rho)g/B]2k(y)$. Conservation of current requires that there be a flow of electric current outside the plume in the direction ($\pm x$) of the applied magnetic field equal to $-[(\Delta\rho)g/B]k_y(y)$. The effect of the buoyancy force is transmitted via these force-free electric currents in both directions along the imposed magnetic field to two images of the plume, located roughly at distances $x = \pm t$ from it. Within these images, a return flow of electric current in the y direction, when crossed with the applied magnetic field, produces an upward force which accelerates the fluid within those images from rest. This provides an inertial force which balances the prescribed buoyancy force (see Figure 4). Diffusive processes are negligible during this phase, provided $1 \ll MP$, as we assume.

The Alfvén waves occur for each value of y for which k, as given by (3.15), is nonzero. The associated velocity w and magnetic-field perturbation c (i.e., the electric-current streamfunction) are as follows.

For $x_L < x < x_R$ (i.e., $|x-h| < k$):

$$w = MPk(y) ; \qquad c = h(y) - x ; \tag{4.3}$$

for $k < |x-h| < t-k$:

$$w = MPk(y) , \qquad c = -\operatorname{sgn}(x)k(y) ; \tag{4.4}$$

for $t-k < |x-h| < t+k$:

$$w = MP[t+k-|x-h|]/2 , \qquad c = -\operatorname{sgn}(x)[t+k-|x-h|]/2 ; \tag{4.5}$$

for $t+k < |x-h|$:

$$w = c = 0 , \tag{4.6}$$

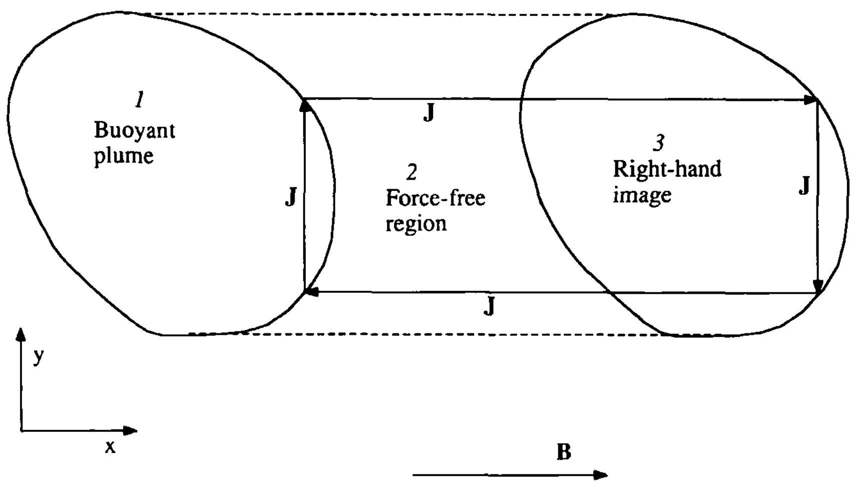

Figure 4 A cartoon of the structure of the two-dimensional Alfvén mode, showing the flow of electric currents and the forces. Region *1* is the buoyant plume and region *3* is an image of the plume which is propagating to the right with the Alfvén speed; a second image (not shown) propagates to the left. The plume image has traversed region *2*. In region *1* the upward buoyancy force is balanced by a downward Lorentz force resulting from a lateral electric current J of (dimensional) density $(\Delta\rho)g/B$ interacting with the applied magnetic field having magnitude B. In region *2*, force-free electric currents flow parallel to the applied magnetic field. The electric circuit is completed by a lateral flow of current in region *3*. This lateral current interacts with the applied field to produce an upward Lorentz force which accelerates the fluid from rest to (dimensional) speed of magnitude $(\Delta\rho)gL(\mu/\rho)^{1/2}/B$. The fluid in regions *1* and *2* rises steadily with speed of that same magnitude.

where x_R and x_L are the right and left portions of the plume boundary given by (3.13) and h is the local center of the plume given by (3.14).

Note that the structure of the velocity (4.4) behind the Alfvén wave is identical to that of the steady state, given by (3.18), except that the order of magnitude differs by a factor P. We shall see that this similarity of velocity structure does not prevail during the intermediate time interval.

These nondiffusive solutions prevail as long as viscous and resistive effects are small. With $P \ll 1$, resistive effects become important first, on a time of order MP. When $t > O(MP)$, an intermediate-time balance between lateral (in the y direction) ohmic diffusion and induction prevails in the magnetic equation, but the viscous term remains small provided $t < O(M/P)$. In this regime, the two-dimensional Alfvén wave solution is strongly modified, but a one-dimensional mode persists, as we shall now show.

4.2 One-dimensional Alfvén mode

Let us consider the problem for the integrated variables

$$W(x,t) = \int_{-\infty}^{\infty} w(x,y,t)dy, \qquad C(x,t) = \int_{-\infty}^{\infty} c(x,y,t)dy\,, \tag{4.7}$$

formed by integration of (2.3) and (2.4) with respect to y. These give

$$M^{-2}W_{xx}-(MP)^{-1}W_t+C_x=0\,, \tag{4.8}$$

$$C_{xx}-MPC_t+W_x=0 \tag{4.9}$$

with conditions

$$C(x,0)=W(x,0)=0$$

and

$$C(\pm 0,t)=-\operatorname{sgn}(x)A/2\,, \qquad W_x(0,t)=0 \tag{4.10}$$

where A is given by (4.2).

The solution of problem (4.8)–(4.10) may be found in Roberts (1967, p. xx). A pair of one-dimensional Alfvén waves propagate along the magnetic field lines from the buoyant region at unit speed. The wave fronts thicken by ohmic diffusion as $(t/MP)^{1/2}$. The viscous term is negligible. Behind the wave fronts

$$C=-\operatorname{sgn}(x)A/2 \qquad \text{and} \qquad W=MPA/2\,. \tag{4.11}$$

The latter result is easily seen from integration of (4.3). These results apparently hold for all time. However, the steady solution has an averaged momentum which is larger by a factor of $1/P$. We will discuss the resolution of this discrepancy in Section 4.4.

4.3 Intermediate-time regime: ohmic diffusion ($MP \ll t \ll M/P$)

As discussed above, the equations valid for intermediate-time, i.e., for $O(MP)<t<O(M/P)$, are

$$w_t=MPc_x\,, \tag{4.12}$$

and

$$c_{yy}+w_x=0\,. \tag{4.13}$$

These equations contain lateral ohmic diffusion, but no viscous diffusion. They may be combined into a single equation

$$MPw_{xx}=-w_{yyt}\,.$$

From this it is apparent that the Lorentz force produces a diffusive-like term in the x direction and that the magnitude of the effective diffusive coefficient MP is large. Thus the Lorentz force introduces an anisotropy in the diffusion of momentum, reminiscent of Taylor dispersion.

Equations (4.12) and (4.13) are to be solved subject to conditions

$$c(\pm 0, y, t) = -\operatorname{sgn}(x)k(y)\,, \qquad c(x, \pm\infty, t) = 0\,,$$
$$\text{and} \qquad w(x, y, 0) = 0\,. \tag{4.14}$$

The first condition is the forcing for the problem, resulting from the balance of buoyancy and Lorentz forces in the momentum equation. Strictly speaking it should be applied at $x = h \pm k$, but since the length scales in the x direction of interest in the present section are large, the application at $x = 0$ introduces a negligible error. The second is a decay condition. The third ignores the velocity generated during the Alfvén-wave phase, on the assumption that the Alfvén waves have travelled a negligibly small distance while $t \leqslant O(MP)$. Note that c is an odd function of x while w is even. The parity of c and w with respect to y is the same as that of k.

Taking the complex Fourier transform in the y direction using

$$\begin{bmatrix} \hat{w}(x,q,t) \\ \hat{c}(x,q,t) \end{bmatrix} = \frac{1}{\sqrt{2\pi}} \int_{-\infty}^{\infty} \begin{bmatrix} w(x,y,t) \\ c(x,y,t) \end{bmatrix} \exp(iqy)\,dy\,, \tag{4.15}$$

equations (4.12)–(4.13) become

$$\hat{w}_t = MP\hat{c}_x\,, \tag{4.16}$$

and

$$\hat{w}_x = q^2\hat{c}\,, \tag{4.17}$$

with conditions

$$\hat{c}(\pm 0, q, t) = -\operatorname{sgn}(x)\hat{k}(q)\,, \qquad \hat{w}(x, q, 0) = 0\,. \tag{4.18}$$

This problem reduces to that for the integrated variables considered in Section 4.2 if $q = 0$; note that $\hat{k}(0) = A/2$.

The solution of problems (4.16)–(4.18) is

$$\hat{w}(x,q,t) = |q|\hat{k}(q)\left[2\sqrt{\frac{MPt}{\pi}}\exp\left(-\frac{q^2x^2}{4MPt}\right) - |qx|\operatorname{erfc}\left(\frac{|qx|}{2\sqrt{MPt}}\right)\right], \tag{4.19}$$

$$\hat{c}(x,q,t) = -\operatorname{sgn}(x)\hat{k}(q)\operatorname{erfc}\left(\frac{|qx|}{2\sqrt{MPt}}\right). \tag{4.20}$$

It may be seen from this solution that if q is of unit order, w is of order $(MPt)^{1/2}$ and decays in the direction of the applied magnetic field on a length scale $X = O(MPt)^{1/2}$. [In the range $X \ll |x|$, the diffuse two-dimensional Alfvén mode prevails; that portion of the solution is not presented.]

Rather than attempting to invert (4.19) and (4.20) for w and c for all values of x, let us concentrate on the value of the flow speed near the plume. Its transform is obtained by setting $x=0$ in (4.19):

$$\hat{w}(0,q,t)=2\sqrt{\frac{MPt}{\pi}}\,|q|\hat{k}(q)\,. \tag{4.21}$$

Let us investigate this further for a circular plume, with

$$k(y)=\sqrt{1-y^2}\,. \tag{4.22}$$

Noting that k is an even function of y and using formula #3.752.2 on p. 419 of Gradshteyn and Ryzhik (1980) we have

$$\hat{k}(q)=\sqrt{\frac{2}{\pi}}\int_0^1 \sqrt{1-y^2}\cos(qy)dy=\sqrt{\frac{\pi}{2}}\,\frac{\mathrm{J}_1(q)}{q}\,. \tag{4.23}$$

Now, for $q>0$,

$$\hat{w}(0,q,t)=\sqrt{2MPt}\,\mathrm{J}_1(q) \tag{4.24}$$

and

$$w(0,y,t)=2\sqrt{\frac{MPt}{\pi}}\int_0^\infty \mathrm{J}_1(q)\cos(qy)dq\,. \tag{4.25}$$

Using formula #6.671.2 on p. 730 of Gradshteyn and Ryzhik (1980) with $\alpha=1$, $\beta=y$ and $\nu=1$, and noting that $\cos[\arcsin(y)]=(1-y^2)^{1/2}$, we have that

$$\begin{aligned} &\text{for } y<1: && w=2\sqrt{\frac{MPt}{\pi}}\,; \\ &\text{for } 1<y: && w=-2\sqrt{\frac{MPt}{\pi}}\,\frac{1}{\sqrt{y^2-1}\,(y+\sqrt{y^2-1})}\,. \end{aligned} \tag{4.26}$$

The inversion of (4.20) for $x=0$ reproduces the boundary condition (4.14).

It may be seen from (4.26) that the vertical speed near the plume is of the order of $(MPt)^{1/2}$ in the time interval $O(MP)<t<O(M/P)$. As $t\to O(MP)$, then $w\to O(MP)$ and $X\to O(MP)$, in agreement with the short-time solution, and as $t\to O(M/P)$, then $w\to O(M)$ and $X\to O(M)$, in agreement with the steady solution. In the latter limit, the lateral viscous shear becomes important. For larger times, the dominant balance is given by the steady solution of Section 3.

The structure of the vertical speed in the intermediate-time regime, shown in Figure 5, is in marked contrast to the two adjacent time regimes in which the flow structure

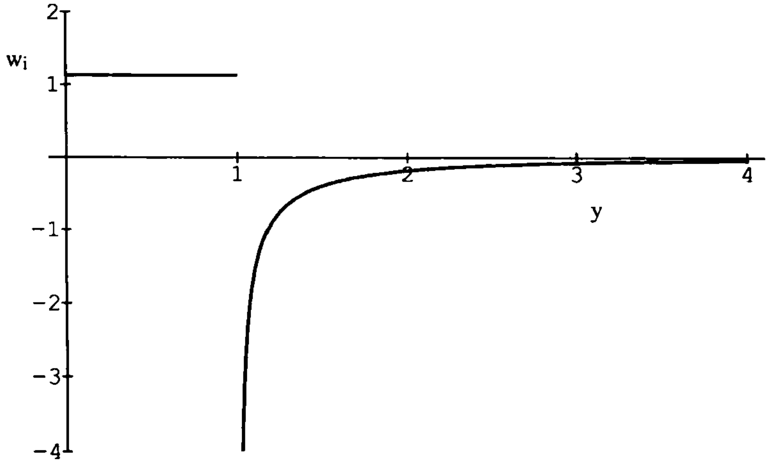

Figure 5 A plot of (4.26) showing the normalized vertical velocity w_i at $x=0$ as a function of lateral distance y in the intermediate-time case for a plume of circular cross-section. Here $w_i = w/(MPt)^{1/2}$. The velocity is symmetric in y and has a zero average in y. The singularity shown here does not occur for other x values.

mirrors that of the buoyant region [see (3.23) and (4.3)]. This solution has several noteworthy properties. First, the velocity is negative for $|y|>1$; although the buoyancy is entirely positive (inducing upward flow), a strong downward flow is induced adjacent to the buoyant region. Furthermore, this velocity is singular at the edge of the buoyant region for $x=0$. (This singularity is not present at $x \neq 0$.) Finally, although the velocity scale $(MPt)^{1/2}$ is of larger order than that of the short-time regime, the solution given by (4.26) is zero when averaged over y. Thus it is not in contradiction with the results of Section 4.2 concerning the averaged properties of the solution.

To understand how a negative velocity may be induced, consider the situation shown in Figure 6, which is to be contrasted with that shown in Figure 4. For time $t > O(MP)$ ohmic diffusion causes the electric currents to diffuse laterally (in the y direction) and to lose their force-free character. The combination of these two effects is to introduce a downward force on the fluid laterally adjacent to the plume, as shown in Figure 6.

It is of interest to determine how the intermediate-time solution found in this subsection merges with the Alfvén solution when $t=O(MP)$ and with the steady solution when $t=O(M/P)$. These merging solutions are developed in the next sub-section.

4.4 Merging solutions

The purpose of this sub-section is to show that the short-time, intermediate-time and steady solutions merge smoothly as time increases. To analyse both cases at once, consider the unsteady equations with only the longitudinal (x-direction) diffusive

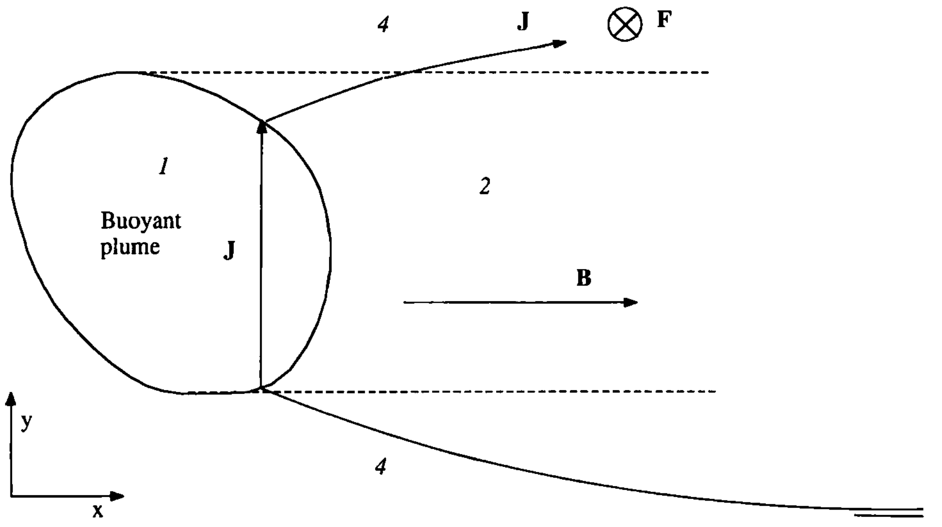

Figure 6 A cartoon of the flow structure near the plume in the intermediate-time case, showing the effect of lateral ohmic diffusion; compare with Figure 4. Electric current diffuses from region *2* into region *4*, where its lateral component interacts with the applied magnetic field to produce a downward Lorentz force. This force induces the negative values of w for $y>1$ shown in Figure 5.

terms being ignored:

$$w_t = MPc_x + (P/M)w_{yy} , \tag{4.27}$$

$$MPc_t = w_x + c_{yy} \tag{4.28}$$

and consider the forcing to be

$$c(\pm 0, y, t) = -\operatorname{sgn}(x)k(y) . \tag{4.29}$$

Taking the Fourier and Laplace transforms of (4.27)–(4.28) yields

$$s\tilde{w} = MP\tilde{c}_x - q^2(P/M)\tilde{w} , \tag{4.30}$$

$$MPs\tilde{c} = \tilde{w}_x - q^2\tilde{c} , \tag{4.31}$$

with

$$\tilde{c}(\pm 0, q, s) = -\operatorname{sgn}(x)\hat{k}(q)/s . \tag{4.32}$$

Here a tilde denotes the double transform and a caret the Fourier transform.

The solution of this problem is

$$\tilde{c}(x,q,s)=-\operatorname{sgn}(x)\left[\frac{\hat{k}(q)}{s}\right]e^{-\lambda|x|}, \tag{4.33}$$

$$\tilde{w}(x,q,s)=-MP\lambda\left[\frac{\hat{k}(q)}{s(s+Pq^2/M)}\right]e^{-\lambda|x|}, \tag{4.34}$$

where

$$\lambda=\sqrt{s+\frac{q^2}{MP}}\sqrt{s+\frac{Pq^2}{M}}. \tag{4.35}$$

Note that the limit as $s\to 0$ of $s\tilde{w}(x,0,s)$ yields $MP\hat{k}(0)$, in agreement with the result of the integrated problem presented in Section 4.2.

The value of w for $x=0$ is of particular interest. Its double transform may be expressed as

$$\tilde{w}(0,q,s)=M\left[\frac{\hat{k}(q)}{s}\right]\sqrt{\frac{MP^2s+Pq^2}{Ms+Pq^2}}. \tag{4.36}$$

Before proceeding with the merging solutions it is helpful to establish that (4.36) reproduces the previous results. First, if $q^2/MP\ll|s|$ (with $P\ll 1$), (4.36) reduces to

$$\tilde{w}(0,q,s)=MP\hat{k}(q)/s. \tag{4.37}$$

The inverse of this is given by the short-time Alfvén solution (4.3). Next, if $q^2P/M\ll|s|\ll q^2/MP$, (4.36) reduces to

$$\tilde{w}(0,q,s)=(MP)^{1/2}q\hat{k}(q)/s^{3/2}. \tag{4.38}$$

The Laplace inverse of this is (4.21). Finally, if $|s|\ll q^2P/M$, (4.36) reduces to

$$\tilde{w}(0,q,s)=M\hat{k}(q)/s. \tag{4.39}$$

which inverts to the steady solution (3.23).

4.4.1. Merging of short-time and intermediate-time solutions

The solution which merges the short-time Alfvén solution (4.3) with the intermediate-time solution (4.26) may be studied by assuming that $|s|=O(q^2/MP)\gg Pq^2/M$. In this limit, (4.36) simplifies to

$$\tilde{w}(0,q,s)=MP\left[\frac{\hat{k}(q)}{s^{3/2}}\right]\sqrt{s+\frac{q^2}{MP}}. \tag{4.40}$$

The Laplace inverse of this is

$$\tilde{w}(0,q,t)=MP\hat{k}(q)G(q^2t/MP) \tag{4.41}$$

where

$$G(z)=e^{-z/2}[(1+z)\mathrm{I}_0(z/2)+z\mathrm{I}_1(z/2)]\ . \tag{4.42}$$

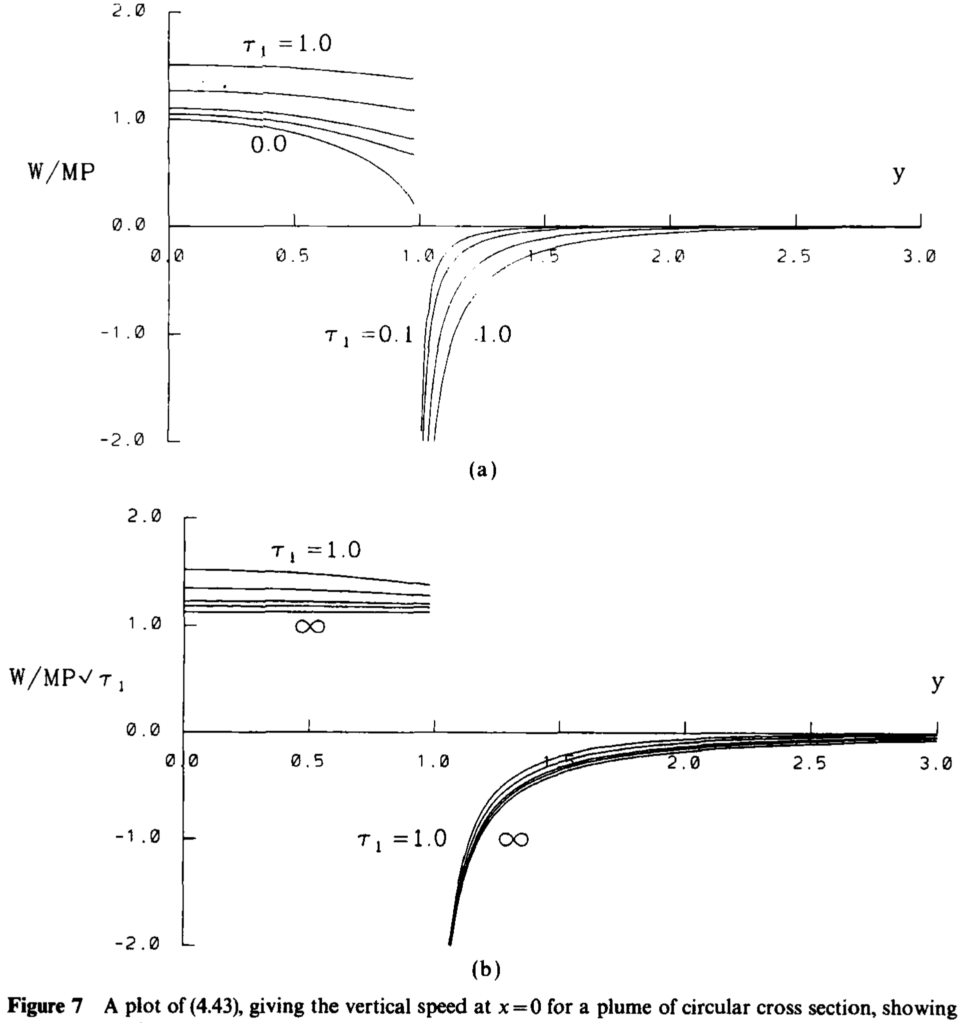

Figure 7 A plot of (4.43), giving the vertical speed at $x=0$ for a plume of circular cross section, showing the merging of the Alfvén solution (4.3) with the intermediate solution (4.26). This is done in two parts due to the different asymptotic scalings. Part 7a shows the normalized vertical velocity w/MP versus y for normalized time $\tau_1=t/MP$ equalling 0, 0.1, 0.2, 0.5 and 1.0, while part 7b shows the normalized velocity $w/MP\sqrt{\tau_1}$ versus y for $\tau_1=1.0$, 2.0, 5.0 and ∞. The curve for $\tau_1=0$ is the solution of (4.3), those labeled $\tau_1=1.0$ in each part are identical, and that labeled $\tau_1=\infty$ is the solution of (4.26). The velocity is symmetric in y.

Let us consider specifically a circular plume. Using (4.23) we have that

$$w(0,y,t)=MP\int_0^{\infty}\left[\frac{J_1(q)}{q}\right]G\left(\frac{q^2t}{MP}\right)\cos(qy)dq\,. \tag{4.43}$$

Figures 7a and 7b show curves of w/MP and $w/MP\sqrt{\tau_1}$ versus y for several values of $\tau_1=t/MP$. This shows the smooth merging of the short-time solution given by

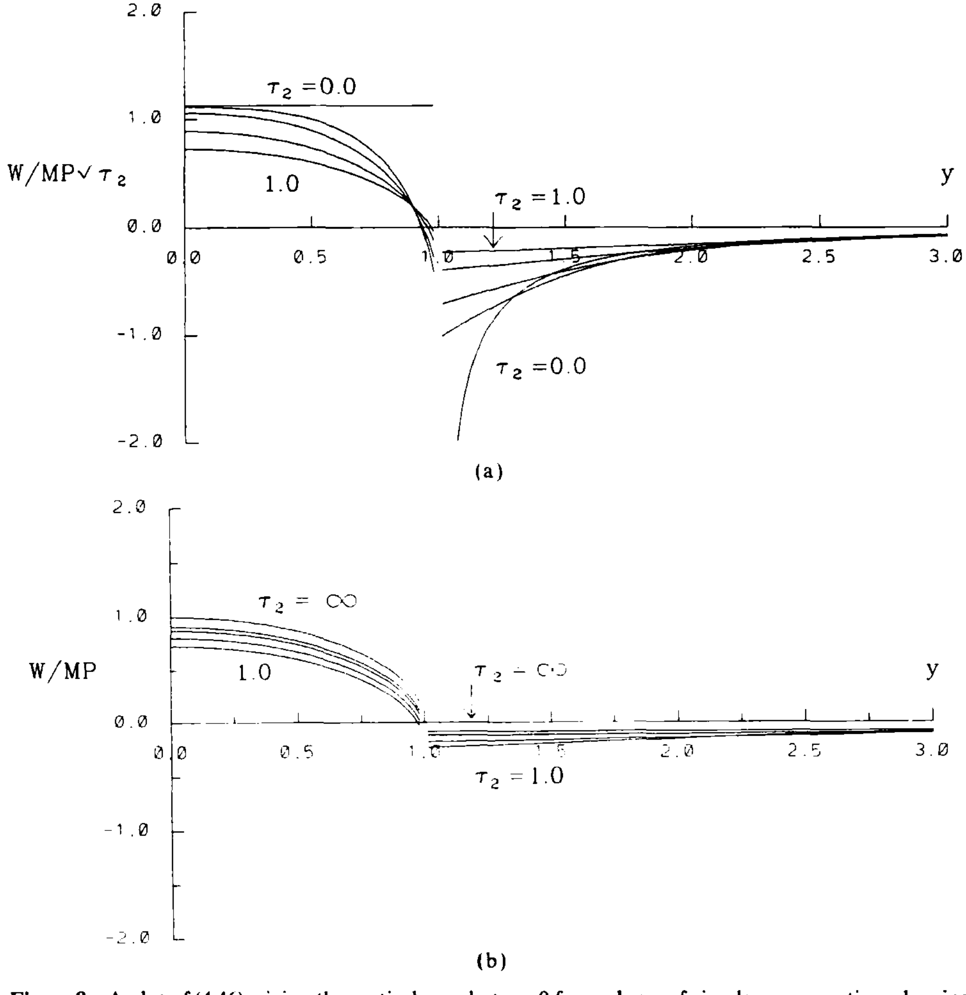

Figure 8 A plot of (4.46), giving the vertical speed at $x=0$ for a plume of circular cross section, showing the merging of the Alfvén solution (4.26) with the intermediate solution (3.19). This is done in two parts due to the different asymptotic scalings. Part 8a shows the normalized vertical velocity $w/M\sqrt{\tau_2}$ versus y for normalized time $\tau_2=Pt/M$ equaling 0, 0.1, 0.2, 0.5 and 1.0, while part 8b shows the normalized velocity w/M versus y for $\tau_2=1.0$, 2.0, 5.0 and ∞. The curve for $\tau_2=0$ is the solution of (4.26), those labeled $\tau_2=1.0$ in each part are identical, and that labeled $\tau_2=\infty$ is the solution of (3.19). The velocity is symmetric in y.

(4.3) with the intermediate-time solution given by (4.26) as τ_1 varies from 0 to ∞. Note that this solution for $x=0$ is singular near $y=1$; this singularity does not occur for other values of x.

4.4.2. Merging of intermediate-time and steady solutions

The solution which merges the intermediate-time solution (4.26) with the steady solution (3.23) may be studied by assuming that $|s|=O(Pq^2/M)\ll q^2/MP$. In this limit, (4.36) simplifies to

$$\tilde{w}(0,q,s)=\left[\frac{q\hat{k}(q)}{s}\right]\frac{\sqrt{MP}}{\sqrt{s+Pq^2/M}}\,. \tag{4.44}$$

The Laplace inverse of this is

$$\hat{w}(0,q,t)=M\hat{k}(q)\,\mathrm{erf}\,(Pq^2t/M)^{1/2}\,. \tag{4.45}$$

Again assuming a circular plume, the Fourier inverse yields

$$w(0,y,t)=M\int_0^\infty \frac{\mathrm{J}_1(q)}{q}\mathrm{erf}\left(q\sqrt{\frac{Pt}{M}}\right)\cos(qy)dq\,. \tag{4.46}$$

Figures 8a and 8b show curves of $w/M\sqrt{\tau_2}$ and w/M versus y for several values of $\tau_2=Pt/M$. This shows the smooth merging of the intermediate-time solution given by (4.26) and the steady solution given by (3.24) as τ_2 varies from 0 to ∞.

5. SUMMARY

We have investigated the steady and transient flow induced by a vertical cylinder of buoyant electrically conducting fluid immersed in an infinite extent of slightly denser fluid in the presence of a horizontal magnetic field. Attention has been concentrated on the rise speed, on its spatial extent and on the dispersion of the momentum added to the system by the buoyant fluid. The sequence of dimensional speeds and spatial scales is as follows.

For very short times [$t<O(L/V_A)$ where $V_A=B/(\rho\mu)^{1/2}$ is the Alfvén speed] the buoyant fluid accelerates from rest: $w=g't$ where $g'=g(\Delta\rho)/\rho$ is the reduced gravity. The non-buoyant fluid remains at rest.

For $t=O(L/V_A)$, Alfvén waves are excited by the accelerated fluid. These waves travel along the field lines with speed V_A.

For short times [$O(L/V_A)<t<O(L^2\mu\sigma)$], the Alfvén waves accelerate the fluid at the wave fronts; diffusion is unimportant. The velocity scale is $w=O(g'L/V_A)$ and the length scale is approximately V_At. The width is determined by the size of the buoyant region.

For $t=O(L^2\mu\sigma)$ lateral ohmic diffusion becomes important and the Alfvén waves give way to a diffusively growing mode. Lateral diffusion of the electric currents induce downward flow adjacent to the buoyant region.

For intermediate times $[\mathrm{O}(L^2\mu\sigma)<t<\mathrm{O}(L^2/\nu)]$ the velocity and its length scale grow as the square-root of time:

$$w_d=\frac{g'}{V_A}\sqrt{\frac{t}{\mu\sigma}}=\frac{(\Delta\rho)g}{B}\sqrt{\frac{t}{\rho\sigma}},$$

$$X=LV_A\sqrt{\mu\sigma t}=LB\sqrt{\frac{\sigma t}{\rho}}.$$

Note that in this regime the rise speed is independent of the size of the plume. The plume width remains of unit order, although the lateral structure changes significantly.

For $t=\mathrm{O}(L^2/\nu)$ lateral viscous diffusion becomes important and the magnitude of the velocity and its length scale cease to grow with time. The region of upward flow begins to diffuse laterally, increasing the width.

For $\mathrm{O}(L^2/\nu)<t$ the flow reaches a quasi-steady state with

$$w_d=\frac{g'L}{V_A\sqrt{\mu\sigma\nu}}=\frac{(\Delta\rho)gL}{B\sqrt{\rho\sigma\nu}},$$

$$X=L^2V_A\sqrt{\frac{\mu\sigma}{\nu}}=L^2B\sqrt{\frac{\sigma}{\rho\nu}}.$$

It should be emphasized that these rise speeds are much greater than that estimated from a balance of buoyancy and Lorentz forces.

Let us consider now why the traditional method of scaling the governing equations failed to yield the correct order of magnitude of the vertical flow in steady state. Within the buoyant region the dominant balance within the momentum equation is between the Lorentz and buoyancy forces. That balance correctly yields the magnitude of the perturbation field $c\approx(\Delta\rho)gL\mu/B$. The balance of magnetic induction and diffusion then yields the velocity scale W_0. However, it is easy to overlook the fact that this represents only the difference of velocity that can occur on the lateral scale of the buoyant region, but in the absence of any rigid boundary, does not determine the magnitude of the velocity.

To determine the magnitude of the velocity, we must consider the balances which occur in the non-buoyant fluid surrounding the plume: between Lorentz and viscous forces in the momentum equation and between magnetic induction and diffusion in the magnetic equation. However, it is crucial to note that the gradient operators in the momentum and magnetic equations (2.1) have a different length scale from that of the Laplacians. The Laplacian operators are dominated by lateral variations on the scale, L, of the plume, but the gradients (in the direction of the applied field) are associated with a much longer scale, X. The balances are $Bc/\mu X\approx\rho\nu w/L^2$ and

$Bw/X \approx c/\sigma\mu L^2$. These directly yield the length scale $X = LM$, where M is given by (2.5), and with c known, we have the velocity scale $w = MW_0$, which is the correct order of magnitude of the upward speed.

One remaining point which is unresolved is the discrepancy in the integrated momentum given by (4.11) and that of the steady state (3.23) which is larger by a factor P. This discrepancy is due to the double limit $t \to \infty$ and $y \to \infty$, or equivalently in the double transforms, $s \to 0$ and $q \to 0$. It may be seen from (4.34) that if we take the limit $q \to 0$ first, then

$$\tilde{w}(0, q, s) \approx MP[\hat{k}(q)/s] , \tag{5.1}$$

which agrees with the averaged results of Section 4.2. On the other hand, if we take the limit $s \to 0$ first, then

$$\tilde{w}(0, q, s) \approx M[\hat{k}(q)/s] , \tag{5.2}$$

which agrees with the results of the steady solution given in Section 3. One may think of a broad region of negative flow occurring at very large times and for very large values of $|y|$ which cancels out the large momentum given by (5.2), giving an averaged value consistent with (5.1).

With the parameter values previously chosen for the Earth's core plus $L \approx 100$ m, we have that $V_A \approx 1.8$ m/s, $g' \approx 3 \times 10^{-7}$ m/s^2, $L/V_A \approx 56$ s ≈ 1 minute, $L^2\mu\sigma \approx 3800$ s ≈ 1 hour, $L^2/\nu \approx 10^9$ s ≈ 30 years, $g'L/V_A \approx 1.7 \times 10^{-5}$ m/s and $g'L/V_A(\mu\sigma\nu)^{1/2} \approx 8.6 \times 10^{-3}$ m/s. If this model were applicable to the core, the flow speed would accelerate from rest to 1.7×10^{-5} m/s in the first minute, stay at that value for the next hour, then grow diffusively for the next 30 years to a terminal speed of 8.6×10^{-3} m/s. However, with these values, it would take the plume only 16 years to rise to the top of the core. Therefore, the terminal state would be irrelevant to the core. The rise speed at the top of the core would be roughly 6×10^{-3} m/s, which is significantly larger than the typically quoted value of 10^{-4} m/s for core speeds. Also, the length of the plume (in the direction of the applied magnetic field) would be 2.5×10^6 m, which is roughly the depth of the outer core.

The estimates in the previous paragraph are for purposes of illustration only. It is not meant to imply that this model is directly applicable to the core. Nonetheless, the calculation is instructive in that is shows that it is dynamically possible to achieve geophysically large speeds in the core with compositionally buoyant plumes having a density excess of only one part in 10^7. Since the velocity scales directly with the density contrast $\Delta\rho$, the effect of differing magnitudes is easily estimated. In particular, if $\Delta\rho$ is 10–100 times smaller than assumed here, the flow speed is more in accord with estimates from secular variation.

The model we have studied here is singular in that the effects of rotation are completely absent. Further studies currently in progress will consider the effect of the Coriolis force on the vertically oriented plume at lower latitudes in the core, as well as buoyant material having more general configurations such as tilted plumes and spherical and irregular blobs.

Acknowledgements

This work was supported by the National Science Foundation through grant #EAR-9116956, and by the North Atlantic Treaty Organization through Collaborative Research Grant #910117; this is contribution 342 of the Geophysical Fluid Dynamics Institute, Florida State University, Tallahassee, FL.

References

Braginsky, S. I., "Magnetohydrodymamics of weakly conducting liquids," *Soviet Physics JETP* **37**, 1005–1014 (1960).

Braginsky, S. I., "Structure of the F layer and reasons for convection in the Earth's core," *Soviet Phys. Dokl.* **149**, 8–10 (1963).

Chester, W., "The effect of a magnetic field on Stokes flow in a conducting fluid," *J. Fluid Mech.* **3**. 304–308 (1957).

Copley, S. M., Giamei, A. F., Johnson, S. M. and Hornbecker, M. F., "The origin of freckles in unidirectionally solidified castings," *Metall. Trans.* **1**, 2193–2204 (1970).

Gans, R., "Viscosity of the earth's core," *J. Geophys. Res.* **77**, 360–366 (1972).

Gradshteyn, I. S. and Ryzhik, I. M., *Tables of Integrals, Series and Products*, Academic Press, New York (1980).

Hasimoto, H., "Steady longitudinal motion of a cylinder in a conducting fluid," *J. Fluid Mech.* **8**, 61–81 (1960).

Lamb, H., *Hydrodynamics*, Dover, New York, 6th Ed (1932).

Lehnert, B., "On the behaviour of an electrically conductive liquid in a magnetic field," *Arkiv Physik* **5**, 69–90 (1952).

Loper, D. E., "Hydromagnetic spin-up of a fluid confined by two flat electrically conducting boundaries," *J. Fluid Mech.* **50**, 609–623 (1971).

Loper, D. E., "Structures of the inner core boundary," *Geophys. Astrophys. Fluid Dynam.* **25**, 139–155 (1983).

Loper, D. E. and Roberts, P. H., "A study of conditions at the inner core boundary of the earth," *Phys. Earth Planet. Inter.* **24**, 302–307 (1981).

Lowes, F. J., "The geomagnetic dynamo—elementary energetics and thermodynamics," *Geophys. Surv.* **7**, 91–107 (1984).

Moffatt, H. K., "Liquid metal MHD and the geodynamo," *Proceedings IUTAM Symposium on Liquid Metal Magnetohydrodynamics*, Kluwer Academic Pub., pp. 403–412 (1989).

Moore, D. W. and Saffman, P. G., "The structure of free vertical shear layers in a rotating fluid and the motion produced by a slowly rising body," *Phil. Trans. Roy. Soc. Lond.* A **264**, 597–634 (1969).

Roberts, P. H., *An Introduction to Magnetohydrodynamics*, Longmans (1967).

Roberts, P. H. and Loper, D. E., "Towards a theory of the structure and evolution of a dendrite layer," in: *Stellar and Planetary Magnetism* (Ed. A. M. Soward), Gordon and Breach, pp. 329–349 (1983).

Shercliff, J. A., "Steady motion of conducting fluids in pipes under transverse magnetic fields," *Proc. Camb. Phil. Soc.* **49**, 136–144 (1953).

Shercliff, J. A., "The flow of conducting fluids in circular pipes under transverse magnetic fields," *J. Fluid Mech.* **1**, 644–666 (1956).